Core energy and Peierls stress of a screw dislocation in bcc molybdenum: A periodic-cell tight-binding study

Ju Li,[1] Cai-Zhuang Wang,[2] Jin-Peng Chang,[3] Wei Cai,[4] Vasily V. Bulatov,[4] Kai-Ming Ho,[2] and Sidney Yip[3,*]
[1]*Department of Materials Science and Engineering, Ohio State University, Columbus, Ohio 43210, USA*
[2]*Ames Laboratory and Department of Physics, Iowa State University, Ames, Iowa 50011, USA*
[3]*Department of Nuclear Engineering, Massachusetts Institute of Technology, Cambridge, Massachusetts 02139, USA*
[4]*Lawrence Livermore National Laboratory, University of California, Livermore, California 94550, USA*
(Received 4 March 2004; published 28 September 2004)

Using a formulation based on anisotropic elasticity we determine the core energy and Peierls stress of the $a_0/2[111]$ screw dislocation in bcc molybdenum at $T=0$. We show that a proper definition of the core energy necessarily involves choosing a reference direction $\hat{\mathbf{a}}$ and a reference radius r_0 in order to describe dislocation dipole rotation and dilatation respectively in the asymptotic expansion of the total energy. The core energy is extracted from atomistic calculations for supercells containing a single dislocation dipole with periodic boundary conditions in a manner that treats fully consistently the effects of image interactions, such that the core energy extracted is invariant with respect to the supercell size and shape, image-sum aspect ratio, and dislocation dipole distance and orientation. Using an environment-dependent tight-binding model we obtain 0.371 eV/Å at $\hat{\mathbf{a}}=\langle 11\bar{2}\rangle$ and $r_0=b$ and 3.8 GPa for the energy of a core with zero polarity and Peierls stress for simple shear in $(\bar{1}10)\langle 111\rangle$, respectively, to be compared to 0.300 eV/Å and 2.4 GPa obtained using an empirical many-body potential for a polarized core. Our results suggest that the large Peierls stress of screw dislocation in Mo is due to the transition from nonplanar to planar core, rather than a direct effect of the equilibrium core polarity.

DOI: 10.1103/PhysRevB.70.104113 PACS number(s): 61.72.Lk, 61.72.Bb, 62.20.Dc, 62.20.Fe

I. INTRODUCTION

The unusual behavior of screw dislocations in bcc metals has long been attributed to its nonplanar core structure,[1–4] with further complications from the possibility of spontaneous polarity,[5] where atomic rows closest to the core center shift in either $\langle 111\rangle$ or $\langle \bar{1}11\rangle$ to break the $\langle \bar{1}10\rangle$ diad symmetry.[6,7] Whether the finite polarity of the equilibrium core has anything to do with the high Peierls stress, in addition to the nonplanarity, is currently a topic of research.[8–15]

Experimentally measured yield stress of single crystal Mo shows strong temperature dependence from 0 to ~400 K,[16] suggesting a significant lattice friction effect. It is commonly believed that in the $\{110\}\langle 111\rangle$ slip system of Mo, nonscrew dislocations have a much higher mobility than the screw dislocations, which move by the double-kink mechanism,[17,18] and whose kinetics is controlled by kink nucleation rather than migration, as the kinks have nonscrew character. Recent calculations have shown that heterogeneous nucleation of kinks from dislocation triple junctions[19] may greatly reduce the kink nucleation stress from that of "homogeneous nucleation" (spontaneous nucleation of double kinks on an infinitely long, straight screw dislocation without the aid of other defects). This may help explain why the Peierls stress calculated for perfect screw dislocation in (110) plane is 0.015 to 0.025G (G is the resolved shear modulus) or 2.1–3.4 GPa,[9,11] whereas the experimentally measured critical resolved shear stress is only ~750 MPa as $T\to 0$ K.[16] Nonetheless, the proper atomistic determination of the core structure, core energy and Peierls stress of an infinitely long straight screw dislocation in Mo is still an important problem at the conceptual and technical levels.[20,21]

Two major sources of errors could arise in a quantitative atomistic study of dislocation core structure and energetics, the accuracy of the interatomic interaction model and the effects of boundary conditions imposed to carry out the calculation. Empirical interatomic potentials, often fitted to equilibrium properties,[22] allow large enough system sizes to be treated; however, there is no assurance they will give realistic results at large strains (see Fig. 1). Density functional theory (DFT), on the other hand, provides accurate energetics, but is limited to small supercells where core over-

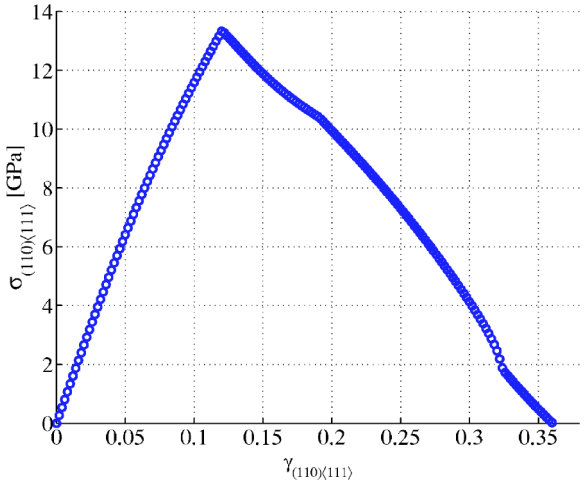

FIG. 1. Relaxed $(\bar{1}10)\langle 111\rangle$ shear affine stress-strain response in Mo calculated using the Finnis-Sinclair potential (Ref. 22). The cusp in the response is due to the finite potential cutoff between the second- and third-nearest neighbors.

lapping and image stress effects can be significant; furthermore, in bcc Mo, **k**-point sampling and energy cutoff convergence needs to be monitored carefully. Added to these concerns are difficulties in extracting the dislocation core energy and Peierls stress from atomistic calculations using the periodic boundary condition (PBC), the problem of "conditional convergence" in the image dislocation dipole summation. One approach circumventing the latter is to use instead the so-called first-principles Greens function boundary condition (FP-GFBC) to study a single dislocation.[11,23] Alternatively, we have developed a formalism for PBC calculations of the core energy[20,21] and the Peierls stress[20,21,24] whose results are manifestly invariant with respect to the image-sum aspect ratio, supercell geometry, and position and direction of the dislocation dipole. This is the approach adopted for the present work.

In Sec. II, we propose a rigorous definition of the dislocation core energy based on a thought experiment of creating an isolated dislocation dipole in an infinite atomistic crystal. The physical significance and mathematical utility of the core energy are discussed. It is shown that in an anisotropic elastic crystal, a reference direction $\hat{\mathbf{a}}$ is needed for the core energy to have a properly defined value, in addition to a reference radius r_0. In Sec. III, we review the procedure that enables one to extract the core energy from PBC supercell calculations, and use the empirical, many-body Finnis-Sinclair potential[22] as a test case to verify the invariance of the results. In Sec. IV, we use an environment-dependent tight-binding potential for Mo (Refs. 25–28) to determine the core energy and Peierls stress of screw dislocation, and compare results with the Finnis-Sinclair potential. The relationship between the equilibrium core polarity and the Peierls stress is also discussed. Finally, a summary is given in Sec. V.

II. MATHEMATICAL DEFINITION AND PHYSICAL MEANING OF DISLOCATION CORE ENERGY

There are two definitions of the dislocation core: a physical core and a mathematical (elasticity) core. The physical core is defined by atoms whose local atomic order like the coordination number or inversion symmetry is drastically different from that of the crystalline bulk, from which we may define a core size r_0^{phys}. Obviously, r_0^{phys} is significant and useful, but needs not be a precise real number due to lattice discreteness. In contrast, the mathematical core radius r_0 and core energy E_{core} can be defined as precise real numbers from an asymptotic expansion of the total energy of a dislocation dipole in an infinite, and otherwise perfect, atomic lattice,

$$E(\mathbf{d}) = 2E_{\text{core}} + 2A(\theta) + \frac{K_s|\mathbf{b}|^2}{2\pi}\log\frac{|\mathbf{d}|}{r_0} + \mathcal{O}(|\mathbf{d}|^{-1}), \qquad (1)$$

at large $|\mathbf{d}|$. Here, $E(\mathbf{d})$ is defined to be the total energy increase in a thought experiment of an infinite discrete lattice whose atoms displace according to the leading-order Stroh solution[29] $\mathbf{u}_G(\mathbf{x})$ at $|\mathbf{x}\pm\mathbf{d}/2| \gg r_0^{\text{phys}}$, but which are allowed to relax atomistically near the physical cores. As the Stroh solution is self-equilibrating (stress equilibrium is satisfied) in the far field, the above thought experiment is well-posed and $E(\mathbf{d})$ is the final increase in the atomistic total energy. At large $|\mathbf{d}|$, the leading **d**-dependent term in $E(\mathbf{d})$ must be $K_s|\mathbf{b}|^2(\log|\mathbf{d}|)/2\pi$, with K_s proven invariant with respect to the displacement cut direction $\hat{\mathbf{d}} \equiv \mathbf{d}/|\mathbf{d}|$.[30] Let us define θ to be the angle between $\hat{\mathbf{d}}$ and an arbitrarily chosen reference direction $\hat{\mathbf{a}}$, with $\hat{\mathbf{d}} \perp \boldsymbol{\xi}$ and $\hat{\mathbf{a}} \perp \boldsymbol{\xi}$, $|\hat{\mathbf{d}}| = |\hat{\mathbf{a}}| = 1$, and $\boldsymbol{\xi}$ is the line direction of the straight dislocation. An asymptotic expansion of $E(\mathbf{d})$ at large $|\mathbf{d}|$ would yield $\mathcal{O}(\log|\mathbf{d}|)$, $\mathcal{O}(1)$, $\mathcal{O}(|\mathbf{d}|^{-1}), \ldots$ terms. The $\mathcal{O}(1)$ term may generally contain a θ-dependent component $2A(\theta)$, and a θ-independent component. For the sake of definiteness, we require $A(\theta=0)=0$, and $\hat{\mathbf{a}}$ will be called the zero-angle reference axis. $A(\theta)$ is entirely given by anisotropic elasticity,

$$2A(\theta) = \sum_{\alpha=1}^{3} \frac{\mathbf{b}^T\mathbf{K}_\alpha\mathbf{b}}{4\pi}\log\frac{(\hat{d}_x + p_\alpha^r\hat{d}_y)^2 + (p_\alpha^i\hat{d}_y)^2}{(\hat{a}_x + p_\alpha^r\hat{a}_y)^2 + (p_\alpha^i\hat{a}_y)^2}, \qquad (2)$$

where $p_\alpha \equiv p_\alpha^r + ip_\alpha^i$, $\alpha = 1, \ldots, 3$, are the three Stroh eigenvalues with nonnegative imaginary parts, and $\mathbf{K}_\alpha \equiv -2[\text{Re}(\mathbf{L}_\alpha)\text{Im}(\mathbf{L}_\alpha)^T + \text{Im}(\mathbf{L}_\alpha)\text{Re}(\mathbf{L}_\alpha)^T]$ is the mode-specific modulus,[30] with $\Sigma_{\alpha=1}^3 \mathbf{b}^T\mathbf{K}_\alpha\mathbf{b} = K_s|\mathbf{b}|^2$. Physically, $2A(\theta)$ is the rotational energy landscape of a dislocation dipole with fixed $|\mathbf{d}|$ in an infinite anisotropic crystal[21] when $|\mathbf{d}|$ is asymptotically large. It is seen from Eq. (2) that $A(\theta) = A(\theta + \pi)$. To illustrate, $A(\theta)$'s for Si $a_0/2[1\bar{1}0]$ shuffle-set screw and Mo $a_0/2[111]$ screw dislocations are evaluated and shown in Fig. 2.

With the $\mathcal{O}(\log|\mathbf{d}|)$ and θ-dependent $\mathcal{O}(1)$ parts known, the $|\mathbf{d}|$- and θ-independent $\mathcal{O}(1)$ part of $E(\mathbf{d})$ can be used to select the mathematical core r_0, E_{core} pair. Imagine for a fixed θ, we plot $E(\mathbf{d})$ data with $|\mathbf{d}|$ on a chart (**d** can only take discrete lattice spacing), and we would like to fit the data to a smooth function $\tilde{E}(\mathbf{d})$. We need to shift the function $K_s|\mathbf{b}|^2(\log|\mathbf{d}|)/2\pi$ up or down to get a good fit at large $|\mathbf{d}|$. That shift operation is well defined asymptotically and is unique. If we ignore $|\mathbf{d}|^{-1}$ etc. terms in the fitting template $\tilde{E}(\mathbf{d}) \equiv 2E_{\text{core}} + 2A(\theta) + (K_s|\mathbf{b}|^2/2\pi)\log(|\mathbf{d}|/r_0)$, $2E_{\text{core}} + 2A(\theta)$ would be the abscissa of $\tilde{E}(\mathbf{d})$ at $|\mathbf{d}| = r_0$. It does *not* mean, however, that $E(r_0) = 2E_{\text{core}} + 2A(\theta)$, as $\tilde{E}(\mathbf{d})$ only fits $E(\mathbf{d})$ well at large $|\mathbf{d}|$ (satisfying at least $|\mathbf{d}| \gg 2r_0^{\text{phys}}$). It is thus clear that r_0, E_{core} (and $\hat{\mathbf{a}}$) are mathematical instruments to fit $E(\mathbf{d})$ to an asymptotic form and do not carry physical meaning in either quantity alone. If one likes, one may choose $r_0 = 1000|\mathbf{b}|$ and select E_{core} accordingly so $\tilde{E}(\mathbf{d})$ remains the same function and nothing is changed. There are several popular choices, however, such as (a) take $r_0 = |\mathbf{b}|$, (b) choose r_0 so $E_{\text{core}} = 0$, (c) $r_0 = r_0^{\text{phys}}$ to minimize confusion, (d) $r_0 = 1$ Å to simplify numerical calculation, etc. It is seen that except for (c), none of the r_0's has anything to do with a physical core size. It is also clear that although $\tilde{E}(\mathbf{d})$ by definition must fit $E(\mathbf{d})$ well at large $|\mathbf{d}|$, there should be a big error as $|\mathbf{d}| \to 2r_0^{\text{phys}}$ and the physical cores begin to overlap. Finally, $\hat{\mathbf{a}}$, r_0, and E_{core} combined do carry physical

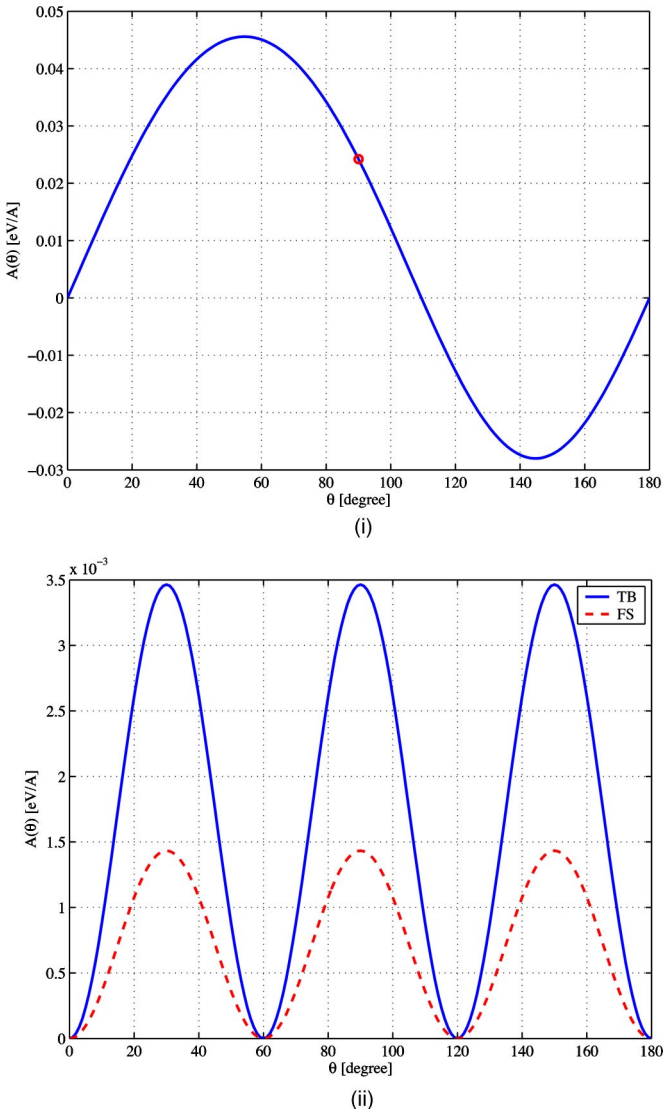

FIG. 2. (Color online) (a) The angular function $A(\theta)$ of $a_0/2[1\bar{1}0]$ shuffle-set screw dislocation in Stillinger-Weber potential Si (Ref. 20), with $\langle 11\bar{2}\rangle$ as the zero-angle reference axis $\hat{\mathbf{a}}$. The corresponding core energy is computed to be 0.502 eV/Å for $r_0=|\mathbf{b}|$. In a separate calculation,[20] with $\langle 111\rangle$ as the zero-angle reference axis, the core energy was computed to be 0.526 eV/Å. The 0.024 eV/Å difference is verified to be exactly $A(\theta=\pi/2)$, as shown above in the circle. (b) The angular function $A(\theta)$ for Mo $a_0/2[111]$ screw dislocation using the Finnis-Sinclair potential (dashed line) and the tight-binding potential (solid line), both with $\hat{\mathbf{a}}$ chosen to be $\langle 11\bar{2}\rangle$. There is $A(\theta)=A(\theta+\pi/3)$ due to crystal symmetry.

meaning—as much as any other defect formation energies—for example, in evaluating the absolute energy needed for creating a large dislocation loop out of a perfect crystal. The atomistically evaluated E_{core} is essential for developing accurate potential energy landscapes for coarse-grained models like nodal dislocation dynamics. It is needed, for example, in determining how much plastic work is converted into heat as versus defect creation for a given dislocation microstructure. In theory, the numerical values of E_{core} (for the same $\mathbf{b}$, $\boldsymbol{\xi}$, $\hat{\mathbf{a}}$, r_0) can be used to determine which core configuration is the ground state when multiple metastable core configurations are found in an atomistic calculation, [21] although in practice this is often unnecessary, because the difference in E_{core} values is trivially related to the total energy difference between calculations with identical supercells. Thus, the main utility of E_{core} is for calibration and information exchange, and to feed coarse-grained models, rather than for analyzing an atomistic calculation itself.

From the above, it is apparent that the choice of the zero-angle reference axis $\hat{\mathbf{a}}$ influences the numerical value of E_{core}, in addition to the choice of the reference radius r_0. This point is not widely appreciated. Indeed, even the existence of the dipole rotational energy landscape $2A(\theta)$ has usually been ignored in the analyses of atomistic modeling results in the literature. Note from Eq. (2) that $A(\theta)$ originates entirely from elasticity. $A(\theta\neq n\pi)$ is generally nonzero for dislocation dipole except screw dislocation dipole in isotropic medium. For example, even edge dislocation dipole in isotropic medium has nonzero $A(\theta)$. E_{core} completely characterizes the net energy consequence of core atomic relaxations, but one must report what elasticity parameters r_0 and $\hat{\mathbf{a}}$ are chosen as the elasticity matching partners. For instance, it was reported previously[20] that E_{core} of $a_0/2[1\bar{1}0]$ shuffle-set screw dislocation in diamond cubic Si was 0.502 eV/Å, with $r_0=|\mathbf{b}|$ and using the Stillinger-Weber potential. Later, a separate, independent calculation gives $E_{\text{core}}=0.526$ eV/Å for the same setup. It is then traced back and determined that while the latter calculation uses $\hat{\mathbf{a}}=\langle 11\bar{2}\rangle$, the former calculation in effect used $\hat{\mathbf{a}}=\langle 111\rangle$. The offset is exactly given by $A(\theta=\pi/2)=0.024$ eV/Å as shown in Fig. 2(a). So both calculations are completely correct, with the only difference in the choice of the zero-angle reference axis $\hat{\mathbf{a}}$ and a trivial conversion of E_{core}'s between them.

To summarize, the numerical value of E_{core} carries no physical meaning unless $\hat{\mathbf{a}}$ and r_0 are specified. The conversion of E_{core} to other $(\hat{\mathbf{a}},r_0)$ "elasticity references" can be performed easily with the understanding that $E(\mathbf{d})$ of Eq. (1), being a physical measurable in a well-posed thought experiment, is invariant, while $\hat{\mathbf{a}}$, r_0, E_{core} are merely parameters in a mathematical partition of its asymptotic behavior. All our E_{core} values below for Mo screw dislocations are based on choosing $r_0=|\mathbf{b}|$ and $\hat{\mathbf{a}}=\langle 11\bar{2}\rangle$.

III. EXTRACTING CORE ENERGY AND PEIERLS STRESS FROM SUPERCELL CALCULATIONS

Even with the tight-binding potential[25–28] and using state-of-the-art supercomputers, to perform calculations with more than 1000 Mo atoms to satisfactory $\mathbf{k}$-sampling convergence still requires nontrivial computational effort. Thus, we first calibrate the error of small supercells using the Finnis-Sinclair potential[22] before embarking on more expensive tight-binding calculations. From these numerical experiments, we verify that the core energy of Mo screw dislocation can be extracted to high accuracy with a 231-atom supercell dipole configuration using our new PBC image-sum formalism.[20,21] The setup is as follows. Define $\mathbf{e}_1=a_0[11\bar{2}]$,

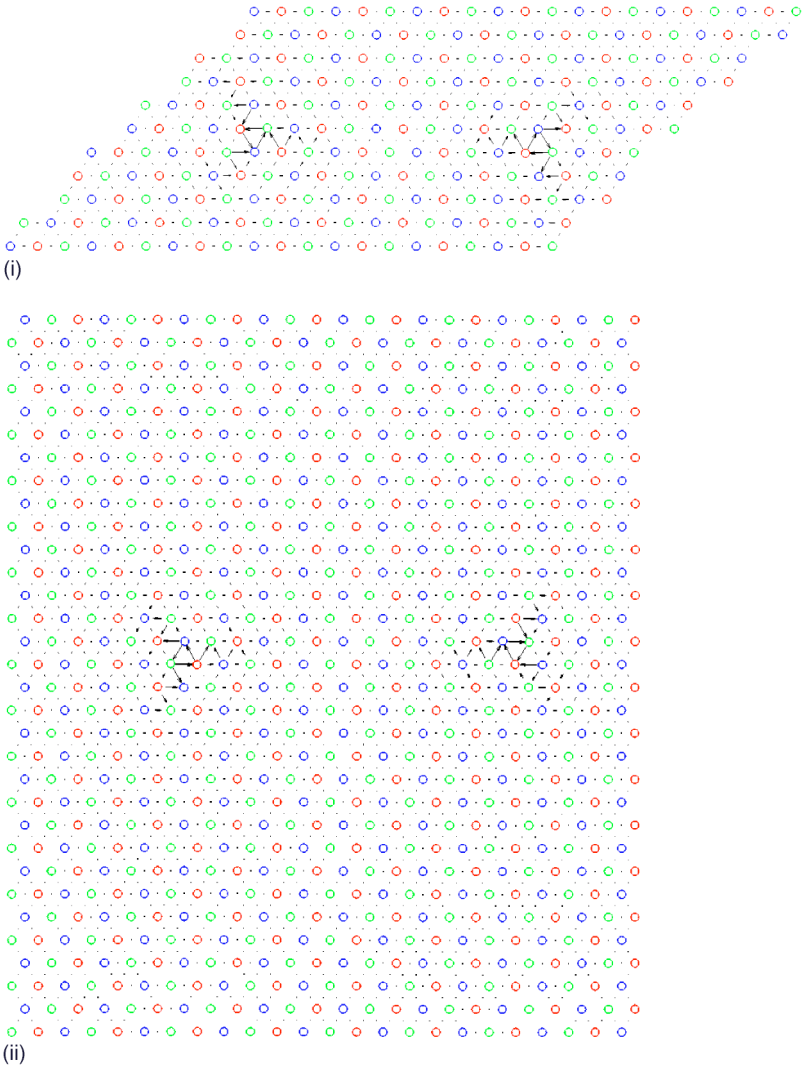

FIG. 3. (Color online) Differential displacement map of Mo screw dislocation using the Finnis-Sinclair potential. (i) $\mathbf{h}_1=7\mathbf{e}_1$, $\mathbf{h}_2=3.5\mathbf{e}_1+5.5\mathbf{e}_2+0.5\mathbf{e}_3$, $\mathbf{h}_3=\mathbf{e}_3$ cell. (ii) $\mathbf{h}_1=8\mathbf{e}_1$, $\mathbf{h}_2=16\mathbf{e}_2+0.5\mathbf{e}_3$, $\mathbf{h}_3=\mathbf{e}_3$ cell.

$\mathbf{e}_2=a_0[\bar{1}10]$, $\mathbf{e}_3=a_0/2[111]$. An orthogonal supercell $7\mathbf{e}_1\times 11\mathbf{e}_2\times\mathbf{e}_3$ is almost square and contains 462 atoms, in which we can put in 4 equally spaced screw dislocations to form a quadrupole.[10,12] Because of symmetry redundancy, this quadrupole cell can be mapped to an entirely equivalent dipole cell half its size [Fig. 3(i)], with three edges $\mathbf{h}_1=7\mathbf{e}_1$, $\mathbf{h}_2=3.5\mathbf{e}_1+5.5\mathbf{e}_2+0.5\mathbf{e}_3$, $\mathbf{h}_3=\mathbf{e}_3$. The $0.5\mathbf{e}_3$ in $\mathbf{h}_2$ is critical in this mapping, in view of the fact that $\epsilon_{\text{total}}=\epsilon_{\text{elastic}}+\epsilon_{\text{plastic}}$, where ϵ_{total} is total strain corresponding to the tilt of the supercell, $\epsilon_{\text{plastic}}$ is the plastic strain generated by the displacement cut in the dipole cell (in the quadrupole cell, $\epsilon_{\text{plastic}}$ is zero as there are two opposing cuts), and $\epsilon_{\text{elastic}}$ is the volume-averaged elastic strain in the supercell, which relates directly to the volume-averaged Virial stress τ_{virial} according to linear elasticity. So, by "preemptively" making $\epsilon_{\text{total}}=\epsilon_{\text{plastic}}$, we make sure that the $\epsilon_{\text{elastic}}=0$ and $\tau_{\text{virial}}\approx 0$. It can be shown that (a) $\tau_{\text{virial}}=0$ minimizes the supercell total energy $E_{\text{atomistic}}$ with respect to the supercell shape $(\mathbf{h}_1,\mathbf{h}_2,\mathbf{h}_3)$,[20,21] and (b) at dipole separation $\mathbf{d}=\mathbf{h}_1/2$, the local stresses at the first and second dislocations vanish simultaneously: $\tau_1=\tau_2=0$. This stabilizes the two dislocations so they do not annihilate, which often happens in small supercell calculations. Even if spontaneous annihilation does not occur, a finite τ_1 or τ_2 would push the dislocation core against the lattice barrier and distort its shape from equilibrium, which would introduce error to the computed core energy E_{core}.

We can now briefly discuss the image sum procedure for extracting the core energy from periodic supercell calculations. A detailed account is given in Ref. 21. An instructive approach to this problem is to think about how to explicitly construct a displacement field $\mathbf{u}(\mathbf{x})$ in the supercell, that (a) satisfies the displacement cut (discontinuity in the displacement field) required by the dipole, (b) is self-equilibrating, and (c) is compatible with the PBC: $\mathbf{u}(\mathbf{x}+\mathbf{h}_i^0)=\mathbf{u}(\mathbf{x})$ and all orders of derivatives including the first, with $\{\mathbf{h}_i^0\}$ being the supercell edges before the dipole cut. The following Green's function sum:

$$\tilde{\mathbf{u}}_\lambda(\mathbf{x}) \equiv \lambda(\mathbf{u}_G(\mathbf{x}) + \sum_{\mathbf{R}\neq 0} \mathbf{u}_G(\mathbf{x}-\mathbf{R})) \tag{3}$$

conceivably could lead to $\mathbf{u}(\mathbf{x})$, where $\mathbf{u}_G(\mathbf{x})$ is the displacement field of an isolated dislocation dipole in an infinite medium (the same one used in the thought experiment of Sec. II). The dislocation lines are all parallel to $\mathbf{h}_3^0$, and $\mathbf{R}=n_1\mathbf{h}_1^0+n_2\mathbf{h}_2^0$, $n_1=-N,\ldots,N$, $n_2=-\alpha N,\ldots,\alpha N$. λ is from 0

to 1 to label the magnitude of the cut displacement from 0 to **b**. Presence of the $\mathbf{u}_G(\mathbf{x})$ term in $\tilde{\mathbf{u}}_\lambda(\mathbf{x})$ will satisfy condition (a). Condition (b) is trivially satisfied as all Green's function displacements are self-equilibrating away from the cores. Condition (c) is a bit more subtle. It can be mathematically proved that,

$$\tilde{\mathbf{u}}_\lambda(\mathbf{x}+\mathbf{h}_i^0)-\tilde{\mathbf{u}}_\lambda(\mathbf{x})=\lambda\mathbf{D}(\alpha)\mathbf{h}_i^0+\mathcal{O}\left(\frac{1}{N}\right) \tag{4}$$

as $N\to\infty$, where $\mathbf{D}(\alpha)$ is a 3×3 affine transformation matrix that depends solely on the image-sum aspect ratio α. $\mathbf{D}(\alpha)$ is the cause of the apparent conditional convergence. To get rid of it, we write

$$\mathbf{u}_\lambda(\mathbf{x})=\tilde{\mathbf{u}}_\lambda(\mathbf{x})-\lambda\mathbf{D}(\alpha)\mathbf{x}. \tag{5}$$

It is seen now that $\mathbf{u}_\lambda(\mathbf{x})$ satisfies (a), (b), (c) simultaneously, so one can use $\mathbf{u}_{\lambda=1}(\mathbf{x})$ to transform atoms in the PBC supercell without creating gaps or stress imbalence. In practice, $\mathbf{D}(\alpha)$ is evaluated numerically by analyzing the behavior of $\tilde{\mathbf{u}}_\lambda(\mathbf{x})$ from image summations at a constant α and progressively large N's.

Suppose we start out with a PBC supercell $\{\mathbf{h}_i^0\}$ containing a stress-free crystal. We adiabatically change λ by effecting a cut increment $d\lambda\mathbf{b}$ along the dipole cut in the cell. At each instant, the displacement field in the cell is $\mathbf{u}_\lambda(\mathbf{x})$, so the stress field $\sigma_\lambda(\mathbf{x})$ is available by plugging in $\nabla\mathbf{u}_\lambda(\mathbf{x})$. The incremental work is simply

$$dW=d\lambda\int\mathbf{b}\cdot\sigma_\lambda(\mathbf{x})\cdot\mathbf{n}dS, \tag{6}$$

which is converted to potential energy. Equations (3), (5), and (6) combined give a total energy expression that consists of:

(1) Dipole self-energy in the form of Eq. (1);
(2) Image dipole/displacement-cut, or dipole-dipole, coupling energy;
(3) $\mathbf{D}(\alpha)$ stress/displacement-cut coupling energy.

Summation over individual Stroh modes in the manner of Eq. (2) is required to account for the dipole-dipole interaction energy $E_{\text{dipole-dipole}}$. The expression

$$E_{\text{dipole-dipole}}=\frac{K_s|\mathbf{b}|^2}{2\pi}\log\frac{|\mathbf{R}+\mathbf{d}||\mathbf{R}-\mathbf{d}|}{|\mathbf{R}|^2} \tag{7}$$

is simply incorrect in anisotropic medium as it ignores the $2A(\theta)$ angle-coupling terms. Note also that one needs to have an extra factor of $1/2$,

$$\Delta W_{\text{image dipole}}=\frac{1}{2}E_{\text{dipole-dipole}} \tag{8}$$

for the $\mathbf{R}\neq0$ dipole-dipole interaction energy, since one dipole "owns" only one-half of the interaction energy. In contrast, it "owns" 100% of its self-energy. All these follow automatically from Eq. (6).

An alternative to the above procedure is to start with the isolated-dipole-in-infinite-medium thought experiment, and add an additional displacement field $\mathbf{w}(\mathbf{x})\equiv\mathbf{u}_{\lambda=1}(\mathbf{x})-\mathbf{u}_G(\mathbf{x})$ to a cut-out region Ω spanned by $\{\mathbf{h}_i^0\}$. Because $\mathbf{w}(\mathbf{x})$ is singularity-free in Ω and self-equilibrating, we can effect that change by dragging the boundary of Ω. The energy increase during this process is simply the boundary work done on $\partial\Omega$ (the outside region $\bar{\Omega}$ needs to be relaxed also, by letting go $\partial\bar{\Omega}$). Furthermore, adding $\mathbf{w}(\mathbf{x})$ in Ω has such an effect that we now can "glue" the opposing sides of $\partial\Omega$ together to produce the self-equilibrating PBC configuration that we seek. In topological terms, we cut a rectangle containing the dipole out of an infinite plane, roll it and stitch it to form a toroidel surface. $\mathbf{w}(\mathbf{x})$ needs to be injected for the edges to match. In this procedure, we bypass integrating over the singularities all together, and the literal implementation of this process actually leads to a viable numerical scheme. But, it has been verified, both analytically and numerically, that the outcome of this procedure is exactly equal to the image dipole sum plus $\mathbf{D}(\alpha)$ work derived nominally from Eq. (6).

Equation (5) setup is easier to explain, but gives a large supercell virial stress, as

$$\epsilon_{\text{plastic}}\equiv\frac{\mathbf{D}_{\text{plastic}}+\mathbf{D}_{\text{plastic}}^T}{2},\quad \mathbf{D}_{\text{plastic}}\equiv\frac{\mathbf{b}(\mathbf{d}\times\mathbf{h}_3^0)^T}{V},$$
$$\epsilon_{\text{elastic}}=-\epsilon_{\text{plastic}} \tag{9}$$

since $\epsilon_{\text{total}}=0$. Therefore in practice we use

$$\mathbf{u}_\lambda(\mathbf{x})=\tilde{\mathbf{u}}_\lambda(\mathbf{x})+\lambda(\mathbf{D}_{\text{plastic}}-\mathbf{D}(\alpha))\mathbf{x} \tag{10}$$

solution, with a new supercell $\mathbf{h}_i=\mathbf{h}_i^0+\lambda\mathbf{D}_{\text{plastic}}\mathbf{h}_i^0$ that is introduced at the beginning of this section. The total energy of this setup can be related to the previous one by accounting for the additional boundary work, which leads to a very simple result.[20,21]

To validate the above, we relax the Mo screw dislocation dipole in four supercell geometries using the Finnis-Sinclair potential:[22]

(i) $\mathbf{h}_1=7\mathbf{e}_1$, $\mathbf{h}_2=3.5\mathbf{e}_1+5.5\mathbf{e}_2+0.5\mathbf{e}_3$, $\mathbf{h}_3=\mathbf{e}_3$ cell, containing 231 atoms;
(ii) $\mathbf{h}_1=8\mathbf{e}_1$, $\mathbf{h}_2=16\mathbf{e}_2+0.5\mathbf{e}_3$, $\mathbf{h}_3=\mathbf{e}_3$ cell, containing 768 atoms;
(iii) $\mathbf{h}_1=16\mathbf{e}_1$, $\mathbf{h}_2=64\mathbf{e}_2+0.5\mathbf{e}_3$, $\mathbf{h}_3=\mathbf{e}_3$ cell, containing 6144 atoms;
(iv) $\mathbf{h}_1=32\mathbf{e}_1$, $\mathbf{h}_2=32\mathbf{e}_2+0.5\mathbf{e}_3$, $\mathbf{h}_3=\mathbf{e}_3$ cell, containing 6144 atoms.

The differential displacement (DD) maps[33] of (i) and (ii) are shown in Fig. 3, in which the spontaneous polarities[5] are manifest, which is characterized by the breaking of the $\langle\bar{1}10\rangle$ diad symmetry operations.[6,7] If we use Å as the length unit, then we can write

TABLE I. Mo screw dislocation core energy with $r_0=|\mathbf{b}|$ and $\hat{\mathbf{a}}=\langle 11\bar{2}\rangle$ using the Finnis-Sinclair potential (Ref. 22).

	$E_{\text{supercell}}$ (eV)	E_{elastic} (eV)	E_{core} (eV/Å)
(i)	6.0410	7.1361	0.2995
(ii)	7.0069	8.0955	0.3006
(iii)	8.8935	9.9838	0.3003
(iv)	11.0432	12.1318	0.3007

$$E_{\text{supercell}} = E_{\text{elastic}} + 2\left(E_{\text{core}} - \frac{K_s|\mathbf{b}|^2}{4\pi}\log r_0\right)|\mathbf{h}_3^0|, \quad (11)$$

where $E_{\text{supercell}}$ is the increase in the total energy of the PBC supercell compared to the perfect crystal, E_{elastic} is the result of the elastic energy summation without the r_0, E_{core} constants, and also by choosing $\hat{\mathbf{a}}=\langle 11\bar{2}\rangle$ so the $2A(\theta)$ term in Eq. (1) gives no contribution (but its equivalent effects are present in the image dipole coupling energies). $K_s|\mathbf{b}|^2/4\pi$, the single dislocation energy prefactor, is 0.499 eV/Å for the Finnis-Sinclair potential. Numerical results for (i)–(iv) are shown in Table I, respectively. We see that by varying the supercell size and shape, the elastic energy E_{elastic} dominates the total energy landscape. However, the differences between $E_{\text{supercell}}$ and E_{elastic} remain remarkably constant. If we take $r_0=|\mathbf{b}|$ and $\hat{\mathbf{a}}=\langle 112\rangle$, then $E_{\text{core}}=0.300\pm0.001$ eV/Å, a definitive result. Thus supercell (i), which contains only 231 atoms, is capable of providing very accurate core energy.

IV. TIGHT-BINDING MODEL RESULTS

The transferable tight-binding model for Mo (Refs. 25–28) used in our calculations has been shown to give the correct band structure, cohesive energy curves for bcc, A15, fcc, hcp, and simple cubic lattices, vacancy and interstitial formation energies, phonon dispersion curve including phonon anomalies at H- and N-points, and (100) surface reconstruction. The equilibrium lattice constant a_0, elastic constants, the $(\bar{1}10)\langle 111\rangle$ and $(11\bar{2})\langle 111\rangle$ resolved shear moduli G, and screw dislocation energy coefficient K_s,[30] are given in Table II, along with the experimental and Finnis-Sinclair potential results.

Numerical experiments of Sec. III indicate that the tilted supercell (i) of 231 atoms would be a good setup for higher-level calculations if the physical core size is comparable to that of the Finnis-Sinclair potential, which turns out to be true with our tight-binding potential[25–28]. In the following calculations we use $1\times1\times28$ **k**-sampling mesh and a Gaussian smearing width of 0.1 eV. We carry out energy minimization with two initial core structures: one freshly generated using Eq. (10) that has no core polarity, and one already fully relaxed by the Finnis-Sinclair potential that has finite polarity as shown in Fig. 3(i). In both cases, it relaxes to the same configuration by the tight-binding potential, with a zero-polarity core structure whose DD map is plotted in Fig. 4(a).

TABLE II. Comparison of equilibrium properties of bcc Mo using the Finnis-Sinclair (Ref. 22) and tight-binding (Ref. 25–28) potentials with experiments (Refs. 31 and 32).

	a_0(Å)	C_{11}(GPa)	C_{12}(GPa)	C_{44}(GPa)	G(GPa)	K_s(GPa)
F-S	3.147	464.7	161.5	108.9	137.4	135.2
TB	3.141	475	145	99	143.0	137.8
Expt.	3.147	479	165	108	140.7	137.9

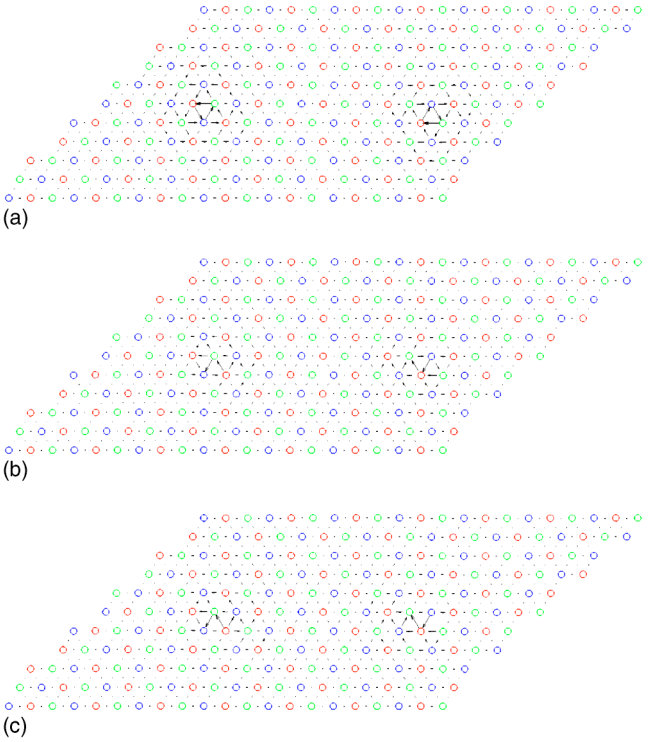

FIG. 4. (Color online) Differential displacement map of Mo screw dislocation using the tight-binding potential. (a) $\tau_1=\tau_2=0$, (b) $\tau_1=\tau_2\approx3.8$ GPa, (c) transient configuration during the stress-driven instability.

The core energy accounting is given in Table III. As the tight-binding potential has slightly different elastic constants from the Finnis-Sinclair potential, the analytic elastic energy sum E_{elastic} is slightly different from that of the Finnis-Sinclair potential (see the first row of Table I), even though the cell geometries are identical. To minimize the error of **k**-sampling, the total energy increment $E_{\text{supercell}}$ is computed with reference to a zero-stress perfect crystal at $\mathbf{h}_1=7\mathbf{e}_1$, $\mathbf{h}_2=3.5\mathbf{e}_1+5.5\mathbf{e}_2$, $\mathbf{h}_3=\mathbf{e}_3$. From E_{elastic} and $E_{\text{supercell}}$ we deduce the core energy E_{core} to be 0.371 eV/Å, which is not very different from the Finnis-Sinclair potential result of 0.300 eV/Å.

TABLE III. Mo screw dislocation core energy with $r_0=|\mathbf{b}|$ and $\hat{\mathbf{a}}=\langle 11\bar{2}\rangle$ using the tight-binding potential (Refs. 25–28).

	$E_{\text{supercell}}$ (eV)	E_{elastic} (eV)	E_{core} (eV/Å)
(i)	6.50704	7.26528	0.37065

Besides the core energy, the formalism outlined in Sec. III also provides a full account of the stress distribution in the cell, local stress τ_1, τ_2 on either of the dislocations leading to Peach-Koehler force, and cell-averaged virial stress τ_{virial}. As a special case, we predict that supercell (i) leads to $\tau_1 = \tau_2 = \tau_{\text{virial}} = 0$. These predictions have been verified explicitly. τ_{virial} is easy to check as it is directly calculable in most atomistic simulation codes. As for τ_1, τ_2, we compare the predictions with numerical results from the so-called local driving force approach,[24] where one evaluates the difference in total energies $\Delta E_{\text{supercell}}$ between two relaxed configurations of identical cell geometries but with one dislocation displaced by one lattice spacing. Both comparisons agree well numerically.

Using cell (i) as a starting point, we may apply additional strain as,

$$\mathbf{h}_1 = 7\mathbf{e}_1,\ \mathbf{h}_2 = 3.5\mathbf{e}_1 + 5.5\mathbf{e}_2 + (0.5 + x)\mathbf{e}_3,\ \mathbf{h}_3 = \mathbf{e}_3, \quad (12)$$

in the tight-binding calculations to study stress-driven instability of the dislocation core. Equation (12) corresponds to simple (unrelaxed) shear in the $(\bar{1}10)\langle 111\rangle$ slip system of bcc Mo. As x is increased, we observe a gradual transition of the screw dislocation core from a threefold symmetric nonplanar structure to one that is more and more localized between two adjacent $(\bar{1}10)$ planes. At a critical value of $x_c \approx 0.24$ [see Fig. 4(b)], we find the core structures can no longer be stabilized and the two cores move toward one another and eventually annihilate, accompanied by large energy drops. A transient configuration is plotted in Fig. 4(c). One may alternatively apply pure (relaxed) shear. In the present setup, the $(\bar{1}10)\langle 111\rangle$ applied shear strain only generates a small $(\bar{1}10)\langle 11\bar{2}\rangle$ parasitic shear stress on the order of 0.8 GPa (0.5 GPa with the Finnis-Sinclair potential), which is too small to induce significant pressure-hardening.[34] So the two loading schemes should give very similar Peierls stress results. Using the $(\bar{1}10)\langle 111\rangle$ resolved shear modulus of $G = 143$ GPa, we estimate that the Peierls stress $\tau_p \approx 0.026G = 3.8$ GPa with our tight-binding potential. In comparison, under the same supercell setup, Finnis-Sinclair potential gives $\tau_p \approx 2.4$ GPa. Using model generalized pseudopotential theory (MGPT),[35] Xu and Moriarty computed τ_p to be ~ 3.4 GPa.[9] Instead of relying on PBC, Woodward and Rao implemented FP-GFBC with planewave ultrasoft pseudopotential DFT and obtained $\tau_p \approx 2.1$ GPa for Mo screw dislocation.[11,23]

Current results suggest that the equilibrium core polarity has no apparent correlation with the high Peierls stress of screw dislocation in bcc Mo.[12] If we regard the Finnis-Sinclair,[22] ultrasoft pseudopotential DFT,[11,23] MGPT,[9,35] and tight-binding models[25–28] as four independent attempts at approximating the true Mo Born-Oppenheimer surface, then an interesting pattern emerges. The first two models give lower τ_p values, but one has a polarized core and the other has a nonpolarized core. Same for the last two models that give higher τ_p values. Therefore, whether τ_p is predicted higher or lower seems to have more to do with other factors in the model than whether the model gives a polarized equilibrium core or not.

On the other hand, all model calculations indicate that in order for bcc screw dislocation to move, it must transform its core structure from having a nonplanar Burgers vector density distribution[36] to a planar distribution. During this process, the polarity order parameter necessarily will change, but perhaps only as a slaved variable to the planarity order parameter.

V. SUMMARY

We have formulated a calculation of the dislocation core energy E_{core} that is mathematically and physically consistent in the framework of anisotropic elasticity. Since a dislocation monopole cannot be created out of an infinite perfect crystal, the core energy is defined through a well-posed thought experiment of creating a dipole. As the total energy of this ideal dipole contains asymptotic elastic-energy terms describing dipole dilatation and rotation, an actual calculation of E_{core} naturally involves the specification of r_0 and $\hat{\mathbf{a}}$. The issue here is similar to choosing a gauge in electrodynamics[37] and choosing solute activity reference states in solution thermodynamics.[38] To our knowledge, this is the first explicit recognition of the nominal angular-dependence in a quantitative determination of E_{core}. After all a dislocation, though analogous to charge in electrodynamics, is not a scalar singularity.

We have shown that with $\hat{\mathbf{a}}$, r_0 specified, E_{core} can be unambiguously extracted from PBC supercell calculations. Using the Finnis-Sinclair potential, we find that a minimal supercell containing 231 atoms and a single dislocation dipole, properly set up, gives a core energy within 1% relative error from the converged result. E_{core}, along with $\hat{\mathbf{a}}$ and r_0, completely characterizes the net energy consequence of core atomic relaxations; this information is critical for developing the total energy landscape of coarse-grained models such as nodal dislocation dynamics.

Using an environment-dependent tight-binding model, we studied the core structure of $a_0/2[111]$ screw dislocation in bcc molybdenum. The core energy of Mo screw dislocation is found to be 0.371 eV/Å at $\hat{\mathbf{a}} = \langle 11\bar{2}\rangle$ and $r_0 = b$, which can be compared to 0.300 eV/Å from the Finnis-Sinclair potential calculation. The equilibrium core structure is found to have zero polarity. The Peierls stress is calculated to be 3.8 GPa, compared to 2.4 GPa for the Finnis-Sinclair potential, when simple shear is applied in $(\bar{1}10)\langle 111\rangle$. Our results suggest that the large Peierls stress of screw dislocation in bcc Mo is due to the nonplanar to planar transition of the core rather than a direct effect of the equilibrium core polarity.

ACKNOWLEDGMENTS

J.L. acknowledges support by Honda R&D Co., Ltd. and the OSU Transportation Research Endowment Program. C.Z.W. would like to thank J. R. Morris for useful discussions. Ames Laboratory is operated for the U.S. Department

of Energy by Iowa State University under Contract No. W-7405-Eng-82. This work was supported by the Director for Energy Research, Office of Basic Energy Sciences including a grant of computer time at the National Energy Research Supercomputing Center (NERSC) in Berkeley; and also performed under the auspices of U.S. Department of Energy by University of California Lawrence Livermore National Laboratory under Contract No. W-7405-Eng-48. J.P.C. and S.Y. acknowledge support by NSF, DARPA/ONR, and Lawrence Livermore National Laboratory.

---

*Electronic address: syip@mit.edu

[1] P. B. Hirsch, in *Proceedings of the Fifth International Conference on Crystallography* (Cambridge University Press, Cambridge, 1960), p. 139.
[2] J. W. Christian, Metall. Trans. A **14A**, 1237 (1983).
[3] M. S. Duesbery, in *Dislocations in Solids*, edited by F. R.N. Nabarro (Elsevier, Amsterdam, 1989), Vol. 8, p. 67.
[4] W. Sigle, Philos. Mag. A **79**, 1009 (1999).
[5] A. Seeger and C. Wuthrich, Nuovo Cimento Soc. Ital. Fis., B **33B**, 38 (1976).
[6] K. Ito and V. Vitek, Philos. Mag. A **81**, 1387 (2001).
[7] V. Vitek, Philos. Mag. **84**, 415 (2004).
[8] M. S. Duesbery and V. Vitek, Acta Mater. **46**, 1481 (1998).
[9] W. Xu and J. A. Moriarty, Comput. Mater. Sci. **9**, 348 (1998).
[10] S. Ismail-Beigi and T. A. Arias, Phys. Rev. Lett. **84**, 1499 (2000).
[11] C. Woodward and S. I. Rao, Philos. Mag. A **81**, 1305 (2001).
[12] G. F. Wang, A. Strachan, T. Cagin, and W. A. Goddard, Phys. Rev. B **67**, 140101 (2003).
[13] D. E. Segall, A. Strachan, W. A. Goddard, S. Ismail-Beigi, and T. A. Arias, Phys. Rev. B **68**, 014104 (2003).
[14] S. L. Frederiksen and K. W. Jacobsen, Philos. Mag. **83**, 365 (2003).
[15] M. Mrovec, D. Nguyen-Manh, D. G. Pettifor, and V. Vitek, Phys. Rev. B **69**, 094115 (2004).
[16] H.-J. Kaufmann, A. Luft, and D. Schulze, Cryst. Res. Technol. **19**, 357 (1984).
[17] A. Seeger, Z. Metallkd, Z. Metallkd. **93**, 760 (2002).
[18] J. Marian, W. Cai, and V. V. Bulatov, Nat. Mater. **3**, 158 (2004).
[19] V. V. Bulatov and W. Cai, Phys. Rev. Lett. **89**, 115501 (2002).
[20] W. Cai, V. V. Bulatov, J. Chang, J. Li, and S. Yip, Phys. Rev. Lett. **86**, 5727 (2001).
[21] W. Cai, V. V. Bulatov, J. Chang, J. Li, and S. Yip, Philos. Mag. **83**, 539 (2003).
[22] M. W. Finnis and J. E. Sinclair, Philos. Mag. A **50**, 45 (1984); **53**, 161(E) (1986).
[23] C. Woodward and S. I. Rao, Phys. Rev. Lett. **88**, 216402 (2002).
[24] J. Li, Ph.D. thesis, Massachusetts Institute of Technology, 2000.
[25] H. Haas, C. Z. Wang, M. Fahnle, C. Elsasser, and K. M. Ho, Phys. Rev. B **58**, 1461 (1998).
[26] H. Haas, C. Z. Wang, K. M. Ho, M. Fahnle, and C. Elsasser, J. Phys.: Condens. Matter **11**, 5455 (1999).
[27] H. Haas, C. Z. Wang, K. M. Ho, M. Fahnle, and C. Elsasser, Surf. Sci. **457**, L397 (2000).
[28] H. Haas, C. Z. Wang, K. M. Ho, M. Fahnle, and C. Elsasser (unpublished).
[29] A. N. Stroh, J. Math. Phys. **41**, 77 (1962).
[30] J. P. Hirth and J. Lothe, *Theory of Dislocations* (Wiley, New York, 1982).
[31] W. B. Pearson, *Handbook of Lattice Spacing and Structures of Metals II* (Pergamon, New York, 1967).
[32] G. Simmons and H. Wang, *Single Crystal Elastic Constants and Calculated Aggregate Properties: A Handbook* (MIT Press, Cambridge, MA, 1971).
[33] V. Vitek, Cryst. Lattice Defects **5**, 1 (1974).
[34] S. Ogata, J. Li, and S. Yip, Science **298**, 807 (2002).
[35] J. A. Moriarty, J. F. Belak, R. E. Rudd, P. Soderlind, F. H. Streitz, L. H. Yang, J. Phys.: Condens. Matter **14**, 2825 (2002).
[36] H. Suzuki, in *Dislocation Dynamics*, edited by A. R. Rosenfield, G. T. Hahn, A. L. Bement, and R. I. Jaffee (McGraw-Hill, New York, 1968), p. 679.
[37] J. D. Jackson, *Classical Electrodynamics*, 2nd ed. (Wiley, New York, 1975).
[38] C. H. P Lupis, *Chemical Thermodynamics of Materials* (North-Holland, New York, 1983).